ISSN 1560-8034, 1605-6582 (On-line), SPQEO, 2019. V. 22, N 2. P. 188-192.

Semiconductor physics

Current-voltage characteristic of the injection photodetector based on M(In)–*n*CdS–*p*Si–M(In) structure

I.B. Sapaev[1], B. Sapaev[2], D.B. Babajanov[3]

[1]*Physical-Technical Institute, Scientific Association "Physics – Sun", Uzbekistan Academy of Sciences, 2B, Bodomzor Yuli str., 100084 Tashkent, Uzbekistan*
[2]*Tashkent State Agrarian University, 2, University Str., 100140 Tashkent, Uzbekistan*
[3]*Turin Polytechnic University in Tashkent, 17, Niyazov Str., 100095 Tashkent, Uzbekistan*
Corresponding author: sapaevibrokhim@gmail.com

Abstract. The current-voltage characteristic of an injection photodiode of the In–*n*-CdS–*p*-Si–In structure, which can operate in a wide spectral range of electromagnetic radiation at room temperature, has been investigated. It is found that the current-voltage characteristic of such structures has a power-law dependence of the current on the voltage. It is shown that in the area of the sharp increase in current of the current-voltage characteristics, participation of defect-impurity complexes in recombination processes becomes decisive.

https://doi.org/10.15407/spqeo22.02.188
PACS 73.40.-c, 85.60.Dw

Keywords: injection, current-voltage, defect-impurity complexes, bipolar drift length, bipolar diffusion length.

Manuscript received 12.11.18; revised version received 07.05.19; accepted for publication 19.06.19; published online 27.06.19.

1. Introduction

There are well known data on formation of injection photodiodes based on A^2B^6 compounds, in particular based on sulfide and cadmium telluride and their solid solutions [1-4]. Ni–*n*-CdS–n^+-CdS structure based on CdS single crystals is considered to have photocurrent strengthening when the structure is illuminated with λ = 0.22 μm light, since there is an injection of the majority charge carriers into a high-resistance *n*-area from the non-illuminated side of n^+-*n* transition [1]. The injection photo-detector with internal strengthening based on cadmium sulfide, capable to operate at room temperature in a wide range of spectrum is not created yet. Such an injection photo-detector with increased output parameters can be created on the *p*-*i*-*n* based structures. For A^2B^6 semiconductors, including CdS, it is technologically difficult to obtain *p*-type conductivity and *p*-*i*-*n* structure on its base because of self-compensation effect. To avoid this problem, we created In–*n*-CdS–*p*-Si–In structure with heterojunction. The high-resistant strongly compensated weak *n*-type CdS layer plays the role of *i*-layer here. The choice of *p*-Si–*n*-CdS heterojunction was previously described in [5].

2. Preparation of samples

The photosensitive In–*n*-CdS–*p*-Si–In structure was created using deposition of CdS layer under the pressure 10^{-5} Torr on the surface of *p*-type silicon plate with the specific resistance $\rho \approx 10$ Ohm·cm and thickness 300 μm. Thus, the CdS source temperature T_{sourse} was maintained at 800…850 °C and substrate (*p*-Si) T_{substr} = 250…300 °C. Observation under the microscope MII-4 showed that CdS films grown on *p*-Si substrate consist of columnar crystallites oriented along the direction of films growth and disorientated on the azimuth direction. We ascertained that the crystallite size was strongly dependent on technological modes and, first of all, on the temperature of Si substrate. For example, CdS films prepared at T_{substr} = 300 °C had the crystallites size close to 3-4 μm and completely penetrated through the film thickness $w \approx 2$ μm. The obtained CdS films were high-resistive, with the specific resistance $\rho = (2…3)\cdot 10^{10}$ Ohm·cm and weak *n*-type conductivity.

The current-collecting Π-shaped contact also was formed by vacuum evaporation of indium.

3. Experimental results and discussion

In Fig. 1, the direct and inverse branches of *j-U* characteristics inherent to the In–*n*-CdS–*p*-Si–In structure are presented in half-logarithmic scale. "+" potential applied to the *p*-Si contact is considered as the forward direction of current in the structure, and with "–" potential – as backward. Our analysis of *j-U* characteristics shows that the structure has rectification properties, and its rectification factor *K* (defined as the ratio of a direct and inverse current at fixed voltage $U = \pm 20$) is approximately 10^5.

The analysis of direct *j-U* characteristics of In–*n*-CdS–*p*-Si–In structures have shown that it consists of four plots at room temperature [6].

The first, second, fourth parts are described by the exponential dependence of current on voltage and have the following analytical form [7]:

$$I = I_0 \exp\left(eU/(ckT) - 1\right), \quad (1)$$

$$c = \left(2b + \mathrm{ch}\left(w/L\right) + 1\right)/\left(b + 1\right), \quad (2)$$

$$c = \left(kT/q\right)\left(b \cdot \mathrm{ch}\left(w/L\right)\right)/\left[2\left(b+1\right) \cdot L \cdot \rho \cdot \tan\left(w/2L\right)\right]. \quad (3)$$

Here, $b = \mu_n/\mu_p$ – electrons to holes mobility ratio, *w* – base thickness, *c* – exponent index, I_0 – pre-exponential multiplier, *e* – electron charge, *k* – Boltzmann constant, *T* – temperature in Kelvins, *U* – bias voltage, *L* – drift length.

Here, we will analyze only the fourth part, since the first, second, and third parts were analyzed in detail in our previous work [6].

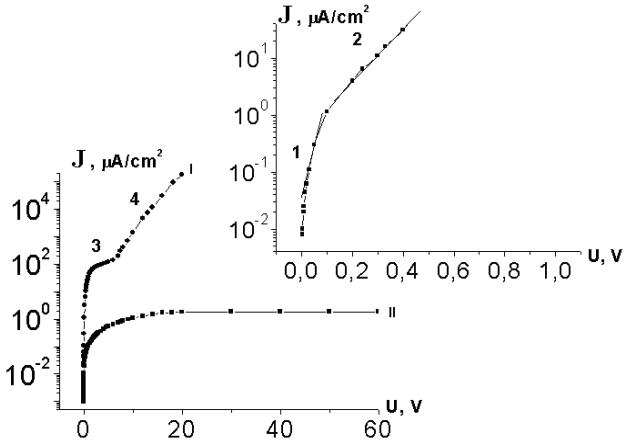

Plots of current-voltage characteristics in semi-logarithmic scale in the dark: (I) forward branch, (II) reverse branch. The third (*3*) and fourth (*4*) parts has been indicated on the forward branches (*I*), while the first (1) and second (*2*) parts has been shown on the forward branches in the plot [6].

As noted above, the fourth part of *j-U* characteristics is defined by the exponential dependence $I = I_{04} \exp\left(qU/kTc_4\right)$, where $c_4 = 2.5$, $j_{04} = 1.9 \cdot 10^{-7}$ A/cm^2. Substituting these experimental data into Exps (2) and (3), we determine the relations of base thickness for the drift length of holes $w/L = 8.5$, and $L = 0.24$ μm, and the resistivity of the base $\rho = 1.9 \cdot 10^7$ Ohm·cm at the values $b = 38$, $w = 2$ μm [8]. The parameters *L* and ρ estimated from the fourth section of the *j-U* characteristic differ significantly from those calculated from the second section of this characteristic. The difference between these values can be explained by a change in the properties of the base with an increase in the current density in the structure. After the sublinear section of the *j-U* characteristic, the recharging of highly compensated recombination centers leads to a decrease in the lifetime of minority carriers, namely, holes. The structure acquires the properties of "long" diodes [9], in which the current is predominantly defined by the drift mechanism. To confirm this assumption, we determined the bipolar diffusion and drift mobilities from the fourth section of the current–voltage characteristic. The experiments demonstrated that the bipolar diffusion length in the fourth section of the forward *j-U* branch is two times less than the value of *L* in the second section of the *j-U* characteristic and is equal to 0.24 μm. In this case, the product μτ decreases by the factor of four. Further, assuming that the mobility and lifetime of the plasma of electron–hole pairs equally decrease by a factor of two, from the expression $L = (D \cdot \tau)^{0.5}$, we find that $D_a = 3.3 \cdot 10^{-1}$ cm$^2 \cdot$s^{-1} for the parameters $L = 0.24$ μm and $\tau = 1.75 \cdot 10^{-8}$ s. Since $D_a = (kT/q)\mu_D$, we found that the mobility of the bipolar diffusion of free carriers $\mu_D = 12.5$ cm^2/V·s. The bipolar drift mobility of free carriers was determined as follows. It was assumed that, in this section of the *j-U* characteristic, the defining current in the structure is the drift one. Therefore, from the values of the voltage and current at the end of the fourth section of the *j-U* characteristic ($U = 20$ V, $j = 0.18$ A/cm^2), we determined the electrical resistivity of the base of the structure. Next, assuming that all the hole-trapping centers ($N_t = 2 \cdot 10^{10}$ cm^{-3}) that play a decisive role in the modulation of the bipolar drift velocity in the sublinear section of the *j-U* characteristic are filled, we find that the concentration of electron–hole plasma is no less than 10^{11} cm^{-3}, which is significantly higher than the concentration of the trapping centers. Then, using the formula $R = \rho d/S$, where $w \approx 2$μm (thickness of the base), ρ is the electrical resistivity of the base, and $S = 0.1$ cm^2 is the active surface area of the structure, we determined the bipolar drift mobility $\mu_a = 112$ cm^2/V·s. It is known that a significant part of the applied potential in the injection diodes drops across the base of the structure.

Therefore, for simplicity, it was assumed that the potential $U = 20$ V applied to the structure is equally distributed between the In–*n*-CdS injecting contact and the base (*n*-CdS). In this case, we have the bipolar drift velocity of holes $v_a = 5.6 \cdot 10^6$ cm/s. For this bipolar drift velocity, we obtain the bipolar drift length of holes $L_{dr} \approx 5.6 \cdot 10^{-2}$ cm for the parameter $\tau \approx 10^{-8}$ s (the lifetime of

the electron–hole plasma), which is more than three orders of magnitude longer than the bipolar diffusion length (L = 0.24 μm). The above performed estimations demonstrate dynamics of increasing the bipolar drift velocity, which completely confirms that, in the fourth section of the current-voltage characteristic, the drift mechanism dominates.

The fourth part of *j-U* curve is also well described by the power law of the type $J \sim U^{\beta}$, where $\beta \approx 6.2$. At sufficiently high injection levels, the concentration of non-equilibrium carriers in In–*n*-CdS strongly increases and, therefore, even in the asymmetric transition it starts playing a prominent role for the second component of current, *i.e*., the drift current [10]. In this case, a decisive role even at the boundary layer, space charge starts playing the carrier drift in the electric field.

The electrical conductivity of the base layer increases more slowly as compared to the increase in the current, and the *j-U* characteristic is described by the power law [6]:

$$I = (9/8)e(n_0 - p_0)\mu_n\mu_p\tau\left(U^{\beta}/w^3\right)S, \quad (4)$$

where n_0, p_0 are the equilibrium concentrations of electrons and holes, μ_n, μ_p – mobilities of electrons and holes, τ is the lifetime of electron-hole plasma, $\beta \approx 2...4$. Further, the product $\mu_n\mu_p \approx 4\cdot10^7$ ($cm^2\cdot V^{-1}\cdot s^{-1}$)^2 was calculated on the basis of equation (4) for the given values: $\rho \approx 2\cdot10^{10}$ Ohm·cm, $n_0 \approx 10^6$ cm^{-3} and μ_n = = 289 $cm^2\cdot V^{-1}\cdot s^{-1}$ [7], and the values of current j = = 0.18 $A\cdot cm^{-2}$ and U = 20 V. Thus, the obtained value of $\mu_n\mu_p$ is larger by four orders than their values according to the literature data [1]. Moreover, this difference is obtained in the case when μ_n = 289 $cm^2\cdot V^{-1}\cdot s^{-1}$ and μ_p = = 8 $cm^2\cdot V^{-1}\cdot s^{-1}$ like to those in single crystals CdS [6]. In addition, the final evaluation indicates that there is conductivity modulation in the base, where the main role is performed by the rapid growth of the bipolar drift mobility of the non-equilibrium carriers with current. This is because the mobility of the bipolar electron-hole plasma, according to [1], is defined as

$$\mu = \frac{n - p\dfrac{dn}{dp}}{n\mu_n + m\mu_p}\mu_n\mu_p, \quad (5)$$

which has a value in the numerator, depending on the difference of concentrations of charge carriers. In the fourth part of the *j-U* curve the change probably occurs in the numerator of Exp. (5) leading to a sharp increase in the mobility of the bipolar electron-hole plasma. The reason may be the levels of adhesion for holes being active.

According to the theory [11], the section of the power current-voltage type $J \sim U^{\beta}$, $\beta > 2$ follows the part of the exponential dependence of the type $J - \exp^{\frac{eU}{ckT}}$ and index of power is not higher than four.

However, due to the structure of the In–*n*-CdS–*p*-Si–In, the plot type $J \sim U^{\beta}$ occurs after the sublinear part of the *j-U* curve and $\beta \approx 6.2$ at the room temperature. This *j-U* curve shape can also be explained in the frame of the theory for the drift mechanism of current transfer, if taking into account the possibility of exchange of free carriers inside a recombination complex. Due to the structure of the In–*n*-CdS–*p*-Si–In, the base is heavily compensated high-resistivity polycrystalline film of cadmium sulfide. Obviously, in these films there may be point defects, such as vacancies of atoms of cadmium (Cd) and sulfur atoms (S). In addition, in the initial powders of CdS compounds, from which the polycrystalline CdS film was obtained, according to technical conditions, there are a few chemical elements: In, Al, Ag, Cu, Fe *etc*. Therefore, forming complexes of various types should be expected in the database (CdS). In the form of compounds, CdS volatile components are the atoms of cadmium. Therefore, in the sublattice of cadmium atoms singly and doubly charged vacancies are easily formed. Doubly charged vacancies of cadmium atoms in most cases form complexes with the positively charged impurity of type $\left(V_{Cd}^{2-}Cd^{+}\right)^{-1}$ and neutral sulfur atoms of type $\left(V_{Cd}^{2-}S^{*}\right)^{-2}$. In addition to these mentioned above, complexes have a large probability of formation of such defect-impurity complexes to negatively "charged acceptor + positively charged ion of introduction" or "positively charged donor + negatively charged vacancy" that can play a decisive role in recombination processes. Therefore, recombination processes in the base of the structure occur not only through simple recombination centers [12] but also through defect-impurity complexes. In this case, the expression for the rate of recombination is undergoing fundamental change and takes the form as follows [11]

$$v = N_R\frac{c_n c_p\left(np - n_i^2\right)}{c_n\left(n - n_i\right) + c_p\left(p - p_i\right) + \alpha\tau_i n p}, \quad (6)$$

where N_R is the concentration of recombination centers (complexes); n, p are concentrations of electrons and holes; n_i is its intrinsic concentration of carriers in the semiconductor; c_n, c_p are the capture coefficients for electrons and holes; n_1, p_1 are equilibrium concentrations of electrons and holes under conditions when the Fermi level coincides with the impurity level (called as static factors by Shockley–Read); τ_i is time taking into account certain processes of electron exchange inside the recombination complex; and β is the coefficient depending on the specific type of impurity or defect-impurity complexes (see [11]).

Despite the different type of complexes, they follow one general pattern – recombination of non-equilibrium electrons and holes with delay, and this inertia of the electron exchange inside the recombination complex

causes the appearance of the latter term in the denominator of Exp. (6). At a sufficiently high level of excitation, it may be crucial. According to the theory [11], areas of *j-U* $J \sim U^{\beta}$, where $\beta > 2$, can be realized when recombination of non-equilibrium current carriers happens with delay, *i.e.*, with participation of complexes for an electronic exchange. In this case, in the denominator of Exp. (6) the following inequality is realized [11]:

$$c_n (n + n_i) + c_p (p + p_i) < \alpha \tau_i n p \tag{7}$$

and *C-U* relationship has the following analytical expression for the structure of *p*-type base [11]:

$$V = \frac{(b+1) w^2 N_R}{b N_a \mu_n \tau_i} + \frac{w \sqrt{J} b}{q \mu_n (b+1) C} + \frac{2(b+1) w^2 N_R c_p}{b N_a \mu_n \beta \tau_i C \sqrt{J}} = \\ = A + B\sqrt{J} - \frac{D}{\sqrt{J}}. \tag{8}$$

Since the investigated structure was created on the basis of the highly compensated cadmium telluride, therefore, the concentration of shallow acceptors $N_A = N_a - N_d$. The parameter C is related with the concentration of electrons at the boundary *n*-CdS – *n*-SiO can be expressed as that in [11]:

$$p(0) = C\sqrt{J} \ . \tag{9}$$

The dependence (7) allows to describe any value of the slope of the *j-U* type $J \sim U^{\beta}$, including the site of sharp growth. A comparison of the backward part of *j-U* dependence $J \sim U^{\beta \approx 4.7...4.8}$ with Exp. (7) allows to determine parameters such as N_R/τ_i, $p(0)$, c_p/α (τ_i is the time delay inside the complex, N_R – concentration of complexes). For this, the equation of a straight line is suitable for the obtained experimental points. For example, making the equation of the straight line for the two experimental points (J_1, U_1 and J_2, U_2) allows determining the value of the voltage [11],

$$U = U_1 - \frac{U_1 - U_2}{J_2 - J_1} J_1 \tag{10}$$

for which it can equate to $A = \frac{(b+1) w^2 N_R}{N_A \mu_n \tau_i}$ from Eq. (8). Further, substituting the values $w = 120$ μm, $b = 10$, $\mu \approx$ ≈ 100 cm^2/V$^{-1}\cdot$s^{-1} and $N_A = 1.5\cdot 10^{10}$ cm^{-3} into (7), we easily define the expression N_R/τ_i. To determine other parameters, the sharp growth of current was chosen by three experimental points (U_1, J_1), (U_2, J_2), (U_3, J_3), for which three equations are applied to determine the coefficients B and D [11]

$$B = \frac{U_2 - U_1}{\sqrt{J_2} - \sqrt{J_1}} - \frac{D\left(\frac{1}{\sqrt{J_1}} - \frac{1}{\sqrt{J_2}}\right)}{\sqrt{J_2} - \sqrt{J_1}}, \tag{11}$$

$$D = \frac{(U_3 - U_2) - (U_3 - U)_2 \frac{\sqrt{J_3} - \sqrt{J_2}}{\sqrt{J_2} - \sqrt{J_1}}}{\left(\frac{1}{\sqrt{J_2}} - \frac{1}{\sqrt{J_3}}\right) - \left(\frac{1}{\sqrt{J_1}} - \frac{1}{\sqrt{J_2}}\right) \frac{\sqrt{J_3} - \sqrt{J_2}}{\sqrt{J_2} - \sqrt{J_1}}} \tag{12}$$

which are then equated to their analytical values given in Eq. (8) allowing to estimate the values $\mu_n C$, $n(0)$, N_R/τ_i and the value $\alpha\tau_i/c_n$ being respectively equal to $N_R/\tau_i =$ $= 3.5\cdot 10^{14}$ cm$^{-3}\cdot$s^{-1}. $n(0)_n = 1.4\cdot 10^{14}$ cm^{-3} and $n(0) =$ $= 1.3\cdot 10^{16}$ cm^{-3}. In this way, specific values of the concentration ratio of the complexes on the delay in complexes and the concentration of the injected non-equilibrium electrons at the beginning and at the end of the segment, the sharp growth of current is reasonable side-altars, as evidenced by the correctness of the assumption. This leads to the conclusion that the recombination processes predominantly involved intrinsic complex systems for the electronic exchange, as a result inertia can appear in the structure. In this case, we are not able to say exactly that complexes are involved in the recombination processes. As was estimated, the value $\alpha\tau_i/c_n = 9\cdot 10^{-10}$ cm is the integral value, where α is a coefficient depending on the specific type of impurity or defect-impurity complexes. In this case, to make full clarity on this issue, it is essential to know the type of complex, which occurs mainly through recombination processes being unknown at the moment.

The direct sequence parts of *j-U* dependence shows that the investigated complex structure and with increasing current density can change the mechanism of current transfer. At low current densities of the resistance, the thickness of the space charge is decisive in the resistance of structures, and the transfer mechanism is the thermionic emission. In the second part of the *j-U* dependence, a significant fraction of the voltage falls on the thickness of the base structure, and the current in structure is restricted by recombination. And, in the recombination processes, defining role is related with simple point recombination centers. The third sublinear part of the *j-U* dependence is characterized by the recombination processes in a large part affected by participation of complex systems; consequently, the lifetime of non-equilibrium carriers is larger than their flight time. This phenomenon leads to change of distribution profile of non-equilibrium carriers resulting in a counter-diffusion and drift flows, which results in appearance of sublinear part in the *j-U* curve. Appearance of the part with a sharp growth of current is obvious that becomes extremely important in the presence of high concentrations of the injected non-equilibrium carriers 10^{14} to 10^{16} cm^{-3} participating in complexes during the recombination processes.

4. Conclusion

An injection photodiode has been created using the In–*n*-CdS–*p*-Si–In structures. The important advantage of the developed structure is that such photodetectors can operate in a wide spectral range of electromagnetic radiation at room temperature. Those photodetectors can be effectively used in optical systems for detecting weak light signals, especially in spectral analyzers for determining the elemental composition of metals and their alloys.

References

1. Vikulin I.M., Kurmashev S.D., Stafeev V.I. Injection photodetectors. *Semiconductors*. 2008. **42**, No 1. P. 113–127. https://doi.org/10.1134/S1063782614100212.
2. Razykov T.M., Kuchkarov K.M., Ferekides C.S., Ergashev B.A., Yuldoshov R.T., Mamarasulov N., Zufarov M.A. Characterization of CdTe thin films with different compositions obtained by CMBD for thin film solar cells. *Solar Energy.* 2017. **144**, No 1. P. 411–416. http://dx.doi.org/10.1016/j.solener.2017.01.047.
3. Mirsagatov S.A., Kabulov R.R., Makhmudov M.A. Injective photo diode with a reconstructed spectrum of photosensitivity based on *n*-*n*/*n*-*n*-hetero-structure. *Semiconductors*. 2013. **47**, Issue 6. P. 825–830. https://doi.org/10.1134/S106378261306016X.
4. Salavei A., Rimmaudo I., Piccinelli F. et al. Influence of CdTe thickness on structural and electrical properties of CdTe/CdS solar cells. *Thin Solid Films*. 2013. **535**. P. 257–260. https://doi.org/10.1016/j.tsf.2012.11.121.
5. Saidov A.S., Leyderman A.Yu., Usmonov Sh.N., Kholikov K.T. *I–V* characteristic of *p–n* structures based on a continuous solid solution $(Si_2)_{1-x}(CdS)_x$. *Semiconductors*. 2009. **43**, No 4. P. 416. https://doi.org/10.1134/S1063782609040022.
6. Mirsagatov Sh.A., Sapaev I.B. Mechanism of charge transfer in injection photodetectors based on the *M*(In)-*n*-CdS-*p*-Si-*M*(In) structure. *Physics of the Solid State*. 2015. **57**, No 4. P. 659–674. https://doi.org/10.1134/S1063783415040162.
7. Jianwei Yan, Yang Chen, Xiaowu Wang, Ying Fu, Juxiang Wang, Jia Sun, Guozhang Dai, Shaohua Tao and Yongli Gao. High-performance ultraviolet photodetectors based on CdS/CdS:SnS_2 superlattice nanowires. *Nanoscale*. 2016. **8**, No 30. P. 14580–14586. https://doi.org/10.1039/c6nr02915a.
8. Fistul V.I. *Physics and Chemistry of the Solid State*. Metallurgiya, Moscow, 1995 (in Russian).
9. Osipov V.V. and Stafeev V.I. *Sov. Phys. Semicond*. 1967. **1**, No 12. P. 1486.
10. Kovalyuk Z.D., Sydor O.M., and Netyaga V.V. Electrical and photoelectrical properties of *n*-InSe/*p*-$CuInSe_2$ optical contact. *Semiconductor Physics, Quantum Electronics & Optoelectronics*. 2004. **7**, No 4. P. 360–362.
11. Leyderman A.Yu., Minbaeva M.K. The mechanism of rapid growth of direct current in semiconductor diode structures. *Fizika Tekhnika Poluprovodnikov*. 1996. **30**, No 10. P. 1729–1738 (in Russian).
12. Mirsagatov Sh.A., Uteniyazov A.K., Achilov A.S. Mechanism of current transport in Schottky barrier diodes based on coarse-grained CdTe films. *Physics of the Solid State*. 2012. **54**, Issue 9. P. 1751–1763. https://doi.org/10.1134/S1063783412090193.

Authors and CV

Bayramdurdy Sapaev defended his Doctoral Dissertation in Physics (Theoretical Condensed Matter Physics) in 2006. Head of the Department of Physics and Chemistry, Tashkent State Agrarian University, Uzbekistan. The area of his scientific interests includes theoretical condensed matter physics.

Doniyor Bahodirovich Babajanov. Research assistant, Turin Polytechnic University in Tashkent, Uzbekistan. His main research field is theoretical Physics. His research interests include nonlinear evolution equations on branched systems and networks, condensed matter physics: particle transport in low-dimensional nano-scale systems and cold atom physics nonlinear dynamics of BEC and vortices.

Ibrokhim Sapaev defended his Ph.D. dissertation in semiconductor physics in 2018 at Physical-technical Institute, Tashkent, Uzbekistan. Senior Researcher of Physical-technical Institute, Tashkent, Uzbekistan. The area of his scientific interests includes semiconductor devices and materials science (diodes, solar cells, nuclear detectors, Si-CdS alloys, Si-CdTe, CVD epitaxy of semiconductor materials), growth of CdS, CdTe, CdO thin films, fabrications, characterizations and testing of device structures based on Si-CdS, Si-CdTe, Si-CdTe-CdS, Si-CdTe-CdO.